

Nuclear Spin, Hyperfine Structure, and Nuclear Moments of 64-Hour Yttrium-90†

F. RUSSELL PETERSEN AND HOWARD A. SHUGART

Department of Physics and Lawrence Radiation Laboratory, University of California, Berkeley, California

(Received August 21, 1961)

The atomic-beam magnetic-resonance method has been used to measure the nuclear spin and hyperfine-structure separations of 64-hour Y^{90} . The results are $I=2$, $a(^2D_{3/2})=-169.749(7)$ Mc/sec, $b(^2D_{3/2})=-21.602(27)$ Mc/sec, $a(^2D_{5/2})=-85.258(6)$ Mc/sec, $b(^2D_{5/2})=-29.716(38)$ Mc/sec. The uncorrected nuclear moments calculated from these measurements are $\mu_I=-1.623(8)$ nm, $Q=-0.155(3)$ b.

I. INTRODUCTION

THE atomic-beam magnetic-resonance method has been used to measure the nuclear spin and hyperfine-structure separations of 64-hr Y^{90} in the $^2D_{3/2}$ and $^2D_{5/2}$ electronic states.¹ Because the apparatus and general technique have been described in detail elsewhere,² only a brief summary of the method is given here.

Yttrium has a $4d5s^2$ electronic ground-state configuration. Because the resulting $^2D_{3/2}$ state is separated by only 530.36 cm^{-1} from the $^2D_{5/2}$ electronic ground state,³ both states are approximately equally populated at the temperatures required to produce an atomic beam. The atomic g factors have been previously measured for the stable isotope by the atomic-beam method with the following results⁴:

$$g_J(^2D_{3/2})=-0.79927(11), \quad g_J(^2D_{5/2})=-1.20028(19).$$

The nuclear spin,^{5,6} nuclear magnetic moment,⁷ and hyperfine-structure separations⁸ for stable Y^{89} are also known very accurately.

This store of knowledge about the electronic and nuclear properties of Y^{89} invited interest in the investigation of the radioactive isotopes. Experimentally, the availability of very pure yttrium metal made pile-produced Y^{90} the most feasible first radioactive isotope for an atomic-beam investigation. Since $I=\frac{1}{2}$ for Y^{89} , investigation of the hyperfine structure of Y^{90} has yielded the first measured quadrupole moment for an yttrium isotope.

II. THEORY OF THE EXPERIMENT

A free atom of yttrium may be represented in an external magnetic field \mathbf{H} by the Hamiltonian

$$\mathcal{H} = (ha\mathbf{I} \cdot \mathbf{J}) + hb \left[\frac{3(\mathbf{I} \cdot \mathbf{J})^2 + \frac{3}{2}(\mathbf{I} \cdot \mathbf{J}) - I(I+1)J(J+1)}{2I(2I-1)J(2J-1)} \right] - (g_J\mu_0\mathbf{J} \cdot \mathbf{H}) - (g_I\mu_0\mathbf{I} \cdot \mathbf{H}), \quad (1)$$

where a and b are the hfs interaction constants, \mathbf{I} and \mathbf{J} are the nuclear and electronic angular momenta in units of \hbar , and μ_0 is the absolute value of the Bohr magneton. The electronic and nuclear g factors are defined by $g_J=\mu_J/J$ and $g_I=\mu_I/I$ where both moments are in units of Bohr magnetons. In the absence of an external magnetic field, the term energies resulting from this Hamiltonian are given by

$$W_F = \frac{haC}{2} + \frac{hb}{4} \frac{\frac{3}{2}C(C+1) - 2I(I+1)J(J+1)}{I(2I-1)J(2J-1)}, \quad (2)$$

where

$$C = F(F+1) - J(J+1) - I(I+1), \quad (3)$$

and

$$\mathbf{F} = \mathbf{I} + \mathbf{J}. \quad (4)$$

In the presence of a magnetic field, a closed-form solution of the secular equation resulting from this Hamiltonian is, in general, not possible. As a result, a computer routine (for the IBM 650) was used to obtain numerical solutions for the term energies as a function of the magnetic field.⁹ A second routine called HYPERFINE (for the IBM 704) was used to fit the experimental data to theory.¹⁰ A useful feature of the HYPERFINE routine is its capacity to fit any combination of the four variables a , b , g_J , and g_I to the experimental data. The fit is obtained by minimizing the χ^2 function defined by

$$\chi^2(a, b, g_J, g_I) = \sum_i [R^i]^2 \omega^i, \quad (5)$$

† This research was supported in part by the U. S. Air Force Office of Scientific Research and the U. S. Atomic Energy Commission.

¹ F. R. Petersen and H. A. Shugart, *Bull. Am. Phys. Soc.* **4**, 452 (1959), and **5**, 504 (1960).

² J. P. Hobson, J. C. Hubbs, W. A. Nierenberg, H. B. Silsbee, and R. J. Sunderland, *Phys. Rev.* **104**, 101 (1956).

³ William F. Meggers and H. N. Russell, *J. Research Natl. Bur. Standards* **2**, 745 (1929).

⁴ Siegfried Penselin, *Z. Physik* **154**, 231 (1959).

⁵ M. F. Crawford and N. Olson, *Phys. Rev.* **76**, 1528 (1949).

⁶ H. Kuhn and G. K. Woodgate, *Proc. Phys. Soc. (London)* **A63**, 830 (1950).

⁷ E. Brun, J. Oeser, H. H. Staub, and C. G. Telschow, *Phys. Rev.* **93**, 172 (1954).

⁸ G. Fricke, H. Kopfermann, and S. Penselin, *Z. Physik* **154**, 218 (1959).

⁹ Hugh L. Garvin, Thomas M. Green, Edgar Lipworth, and William A. Nierenberg, *Phys. Rev.* **116**, 393 (1959). Described in Appendix I.

¹⁰ Reference 9. Modification of the routine described in Appendix II.

according to a procedure developed by Nierenberg.¹¹ The residual, R^i , is given by

$$R^i = (\nu^i)_{\text{obs}} - X_1^{*i} + X_2^{*i}, \quad (6)$$

where X_1^{*i} and X_2^{*i} are the term energies of levels defined by the quantum numbers F_1^i, m_1^i and F_2^i, m_2^i , respectively. The term energies are obtained by solving numerically the secular equation corresponding to the hyperfine Hamiltonian rewritten for this purpose, as

$$\frac{\mathcal{H}}{h} = (a\mathbf{I} \cdot \mathbf{J}) + b \left[\frac{3(\mathbf{I} \cdot \mathbf{J})^2 + \frac{3}{2}(\mathbf{I} \cdot \mathbf{J}) - I(I+1)J(J+1)}{2I(2I-1)J(2J-1)} \right] + \left[\frac{(-g_J + g_I)\mu_0 H J_z}{h} \right] - \left[\frac{g_I \mu_0 H F_z}{h} \right]. \quad (7)$$

The principal g_I dependence can be expressed by

$$X^* = X - (mg_I \mu_0 H / h), \quad (8)$$

where X is the term energy when the last term in the Hamiltonian, Eq. (7), is neglected. The weighting factor, ω^i , is the reciprocal of the sum of the squares of the frequency uncertainties due to resonance linewidth and magnetic-field uncertainty.

Theoretical expressions for the interaction constants are given for a d electron, for example, by Kopfermann.¹² They are

$$a(\text{in Mc/sec}) = \frac{2\mu_0^2 g_I}{10^6 h} \frac{L(L+1)}{J(J+1)} \langle 1/r^3 \rangle_{\text{av}} F_r(J, Z_i), \quad (9)$$

$$b(\text{in Mc/sec}) = \frac{e^2 Q(2J-1)}{10^6 h(2J+2)} \langle 1/r^3 \rangle_{\text{av}} R_r(L, J, Z_i). \quad (10)$$

Here, L is the electronic orbital angular momentum in units of \hbar , Q is the nuclear electric quadrupole moment in cm², e is the electronic charge, and $F_r(J, Z_i)$ and $R_r(L, J, Z_i)$ are relativistic correction factors. The factor $\langle 1/r^3 \rangle_{\text{av}}$ can be estimated from the fine-structure splitting, δ , in the doublet from the expression

$$\langle 1/r^3 \rangle = \frac{hc\delta}{2\mu_0^2 (L + \frac{1}{2}) Z_i H_r(L, Z_i)}, \quad (11)$$

where c is the velocity of light in cm/sec, Z_i is the effective nuclear charge number, and $H_r(L, Z_i)$ is a relativistic correction factor. For radioactive isotopes, uncertainties in magnetic-moment calculations resulting from this estimate can usually be avoided by making use of the fact that electronic effects for two isotopes of the same element can, to a good approximation, be considered the same. Thus, because accurate values of the constants for a stable isotope are known, the Fermi-

Segrè-type relation

$$(g_I)_1 = (a_1/a_2)(g_I)_2 \quad (12)$$

can be used. For quadrupole-moment calculations, the same difficulty can be avoided by use of the ratio of the interaction constants. Thus

$$Q = \frac{4g_I \mu_0^2}{e^2} \frac{F_r(J, Z_i)}{R_r(L, J, Z_i)} \frac{L(L+1)}{J(2J-1)} \frac{b}{a}. \quad (13)$$

In the foregoing theory, it has been assumed that electronic states are not mixed. Schwartz¹³ has considered the effect of electronic configuration mixing on the hfs interaction constants for electronic configurations of the type $s^2 l j$ (or $s^2 l^{-1} j$). The particular case in which one of the s electrons is raised to a higher s state, s' , is considered. The resulting effect can be expected to change the magnetic-dipole interaction constants considerably, but have very little effect on the fine-structure separation and the quadrupole interaction constants.

A procedure is outlined for correcting the dipole interaction constants if experimental measurements in both electronic states of the doublet are available. If a_0 is the corrected constant, then

$$a' = a_0' + \delta', \quad (14)$$

$$a'' = a_0'' + \delta'', \quad (15)$$

$$\frac{a_0'}{a_0''} = \frac{1}{\theta} \frac{J-1}{J+1}, \quad (16)$$

$$\delta' = -\delta'', \quad (17)$$

where

$$\theta = \frac{F_r''}{F_r'} \left| \frac{C''}{C'} \right|^2 \approx 1. \quad (18)$$

Here, primed quantities signify the $J = L + \frac{1}{2}$ state, and double-primed quantities signify the $J - 1 = L - \frac{1}{2}$ state.

III. ISOTOPE PRODUCTION AND IDENTIFICATION

Yttrium-90 was produced from 99.9% pure yttrium metal by the reaction $Y^{89}(n, \gamma)Y^{90}$. Each sample, consisting of approximately 250 mg of metal, was bombarded for about 60 to 120 hr with a flux of $(2 \text{ to } 9) \times 10^{13}$ neutrons/cm²-sec. Irradiations were done initially in the Livermore Pool-Type reactor, and later in the General Electric test reactor at the Vallecitos Atomic Laboratory. Enough activity was produced to allow successful experimenting for periods of from two to three half lives.

Yttrium-90 β^- decays more than 99% of the time to the 0⁺ ground state of Zr⁹⁰ with a 64.2-hr half-life.^{14,15} The radioactive atomic beam was detected by collecting

¹³ Charles Schwartz, Phys. Rev. **97**, 380 (1955).

¹¹ William A. Nierenberg, University of California Radiation Laboratory Report UCRL 3816, 1957 (unpublished).

¹² Hans Kopfermann, *Nuclear Moments*, English version by E. E. Schneider (Academic Press Inc., New York, 1958), 2nd ed.

¹⁴ D. Strominger, J. M. Hollander, and G. T. Seaborg, Revs. Modern Phys. **30**, 585 (1958).

¹⁵ For example, Herbert L. Volchok and J. Lawrence Kulp, Phys. Rev. **97**, 102 (1955).

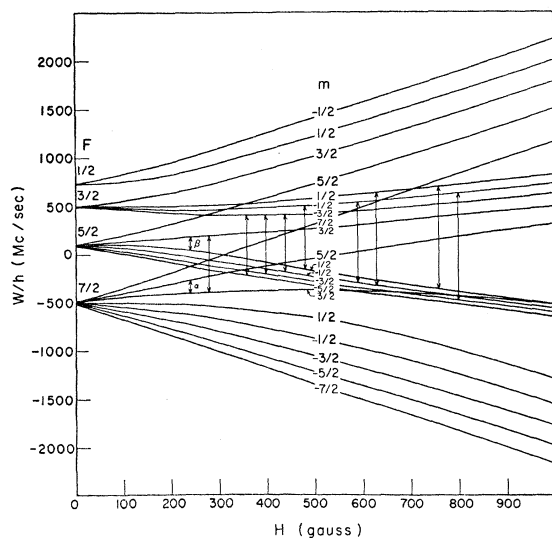
atoms on sulfur-coated surfaces, or "buttons," which were later counted in continuous-flow methane beta counters. Resonance signals were about 30 counts/min above a 10-count/min apparatus background. Typical counter background rates were about 2.5 counts/min. Samples collected at the peak of each resonance were decayed over periods of from three to four half-lives to verify identity of the radioactivity.

IV. EXPERIMENTAL PROCEDURE

We used the general experimental procedure for nonalkali radioactive atomic beams, as described by Ewbank *et al.*,¹⁶ so only a description of techniques peculiar to this isotope is given here.

In principle, the *A* and *B* deflecting fields of a flop-in apparatus focus on the detector only those atoms which change the signs of their effective magnetic moments while the atoms traverse the region between the *A* and *B* magnets. At high *A* and *B* fields, the refocusing condition is satisfied for $m_J = \pm \frac{1}{2} \leftrightarrow \mp \frac{1}{2}$ transitions. For $I = 2$ and normal-level ordering, 11 transitions in the $^2D_{3/2}$ state and 10 transitions in the $^2D_{5/2}$ state are observable. Figures 1 and 2 show these transitions for the case of a negative nuclear magnetic moment.

The yttrium beam was produced from a tantalum oven heated by electron bombardment. A typical oven load consisted of approximately 40 mg of the reactor-irradiated metal contained in a sharp-edged tantalum crucible. Application of about 200 w of oven power, with an oven slit width of 4 mils, produced undeflected beam intensities at the detector position of 200 to 300 counts/min for 1-min exposures. When the inhomogeneous



given by

$$\nu = \nu_\infty + \left\{ \left[\frac{f_1(I, J, g_J)}{\Delta\nu_{F+1, F}} + \frac{f_2(I, J, g_J)}{\Delta\nu_{F, F-1}} \right] H^2 \right\}, \quad (20)$$

where $f_1(I, J, g_J)$ and $f_2(I, J, g_J)$ can be evaluated from second-order perturbation theory. When the shift $(\nu - \nu_\infty)$ became appreciable, preliminary values of the hyperfine-structure separations between the F levels were calculated. These values and Eq. (2) enabled us to obtain preliminary values for the interaction constants a and b . These starting values were then used in the routine HYPERFINE to obtain the best fit to the experimental data.

Observation of the $\Delta F = 0$ transitions was continued to higher magnetic fields until the uncertainty in the predicted frequency for the $\Delta F = \pm 1$ transitions became less than 5 Mc/sec. Initially, the $\Delta F = \pm 1$ searches were performed at low magnetic fields. After observation of several of these transitions, the uncertainties in the interaction constants became small enough to predict high-field $\Delta F = \pm 1$ transitions to within several hundred kc/sec. It was observed that the field dependence, $\partial\nu/\partial H$, of several of these transitions became zero for particular values of H . Since inhomogeneity in the magnetic field was the principal reason for line broadening with this apparatus, the $\partial\nu/\partial H = 0$ points were used to obtain the best values for a and b .

From Eq. (8) we see that the frequency of each transition involves the term

$$-(m_1 - m_2)g_I\mu_0 H/h.$$

For σ transitions ($\Delta m = 0$), this term is zero; consequently, these transitions are much less g_I -dependent than π transitions ($\Delta m = \pm 1$). If the nuclear magnetic moment is appreciable, one would expect the π -transition frequency based on true interaction constants to be measurably different for an assumed positive or negative moment at high magnetic fields. This technique

TABLE I. The most field-independent positions of the observable $\Delta F = \pm 1$ transitions in the $^2D_{3/2}$ electronic state of Y⁹⁰. The calculations were performed for $a = -169.749$ Mc/sec and $b = -21.602$ Mc/sec. The symbols g_I+ and g_I- indicate an assumed positive and negative magnetic moment, respectively.

Transition ($F_1, m_1 \leftrightarrow F_2, m_2$)	$(\partial\nu/\partial H)_{\min}$ (Mc/sec-gauss)	H (gauss)	$\nu(g_I+)$ (Mc/sec)	$\nu(g_I-)$ (Mc/sec)
$\frac{5}{2}, \frac{3}{2} \leftrightarrow \frac{7}{2}, \frac{3}{2}$	0	263.3	589.909	589.909
$\frac{3}{2}, -\frac{1}{2} \leftrightarrow \frac{5}{2}, \frac{1}{2}$	0	127.1	379.885	379.728
$\frac{3}{2}, \frac{1}{2} \leftrightarrow \frac{5}{2}, \frac{3}{2}$	0	191.7	363.144	363.144
$\frac{3}{2}, \frac{1}{2} \leftrightarrow \frac{5}{2}, -\frac{1}{2}$	0	{ 96.6 } { 114.4 }	{ 424.679 } { 424.628 }	{ 424.799 } { 424.770 }
$\frac{3}{2}, -\frac{3}{2} \leftrightarrow \frac{5}{2}, -\frac{1}{2}$	0	19.9	409.618	409.593
$\frac{3}{2}, -\frac{1}{2} \leftrightarrow \frac{5}{2}, -\frac{3}{2}$	0.064	27.0	412.879	412.879
$\frac{3}{2}, -\frac{3}{2} \leftrightarrow \frac{5}{2}, -\frac{5}{2}$	0.288	0	410.871	410.871
$\frac{3}{2}, -\frac{1}{2} \leftrightarrow \frac{5}{2}, -\frac{3}{2}$	0.426	47.5	432.389	432.443
$\frac{3}{2}, -\frac{3}{2} \leftrightarrow \frac{5}{2}, -\frac{5}{2}$	0.703	0	410.871	410.871

TABLE II. The most field-independent positions of the observable $\Delta F = \pm 1$ transitions in the $^2D_{3/2}$ electronic state of Y⁹⁰. The calculations were performed for $a = -85.258$ Mc/sec and $b = -29.716$ Mc/sec. The symbols g_I+ and g_I- indicate an assumed positive and negative magnetic moment, respectively.

Transition ($F_1, m_1 \leftrightarrow F_2, m_2$)	$(\partial\nu/\partial H)_{\min}$ (Mc/sec-gauss)	H (gauss)	$\nu(g_I+)$ (Mc/sec)	$\nu(g_I-)$ (Mc/sec)
$\frac{7}{2}, \frac{3}{2} \leftrightarrow \frac{9}{2}, \frac{3}{2}$	0.016	51.5	405.718	405.718
$\frac{5}{2}, \frac{1}{2} \leftrightarrow \frac{7}{2}, \frac{1}{2}$	0	{ 8.6 } { 63.2 }	{ 293.451 } { 289.572 }	{ 293.451 } { 289.572 }
$\frac{3}{2}, -\frac{3}{2} \leftrightarrow \frac{5}{2}, -\frac{1}{2}$	0	32.5	171.408	171.368
$\frac{3}{2}, -\frac{1}{2} \leftrightarrow \frac{5}{2}, -\frac{3}{2}$	0	13.6	194.660	194.660
$\frac{3}{2}, -\frac{1}{2} \leftrightarrow \frac{5}{2}, -\frac{5}{2}$	0	48.8	176.485	176.485
$\frac{3}{2}, -\frac{3}{2} \leftrightarrow \frac{5}{2}, -\frac{5}{2}$	0.576	0	198.287	198.287
$\frac{3}{2}, -\frac{1}{2} \leftrightarrow \frac{5}{2}, -\frac{3}{2}$	0.134	29.9	211.731	211.768

was used to determine the sign of the nuclear moment of Y⁹⁰.

V. RESULTS

Preliminary observations of $\Delta F = 0$ transitions in both electronic states confirmed the expected spin, $I = 2$. Observation of these transitions at high magnetic fields permitted preliminary estimates of the interaction constants. The ratio b/a indicated that the level ordering was normal.

The low-field $\Delta F = \pm 1$ transitions were first observed in the $^2D_{3/2}$ electronic state. During the investigation, a $^2D_{3/2}$ resonance at approximately 410 Mc/sec was accidentally found. A search soon revealed all eight observable transitions in the $^2D_{3/2}$ state as well as the $F, m = \frac{7}{2}, \frac{3}{2} \leftrightarrow \frac{9}{2}, \frac{3}{2}$ transition in the $^2D_{5/2}$ state in this frequency region. Use of this information and of the known interaction constants of Y⁸⁹ allowed observation of all observable transitions within a short period of time.

By utilization of the improved values for the interaction constants, a computer routine predicted the observable transition frequencies as a function of the magnetic field. Tables I and II show where each transition is least field-dependent. Observation of resonances at these field-independent points permitted the most accurate determination of the interaction constants. Figures 3-6 show typical resonances observed at their field-independent points.

In the hairpin geometry used to produce transitions, the atomic beam passed horizontally by one side of a vertical central conductor which was perpendicular to the magnetic C field. Since during transit each atom was exposed to two rf fields parallel to the magnetic field and 180° out of phase, the transition probability for σ transitions passed through a minimum at the resonant frequency.¹⁷ The resulting double-peaked structure, similar to that shown in Figs. 3 and 5, was observed for all σ transitions carefully done at fields where $\partial\nu/\partial H$

¹⁷ Norman F. Ramsey, *Molecular Beams* (Oxford University Press, New York, 1956).

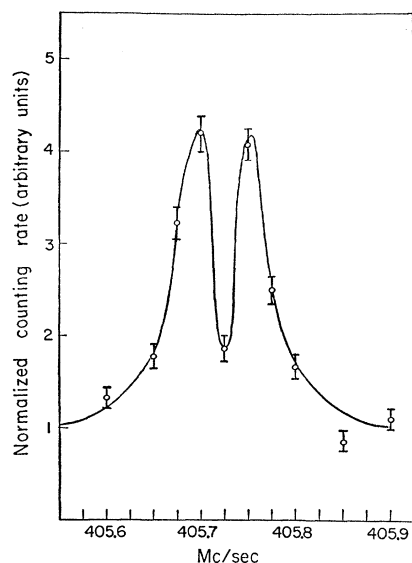


FIG. 3. A resonance corresponding to the transition $F, m = \frac{7}{2}, \frac{3}{2} \leftrightarrow \frac{7}{2}, \frac{3}{2}$ in the $^2D_{3/2}$ electronic state of Y^{90} at $H = 51.4$ gauss.

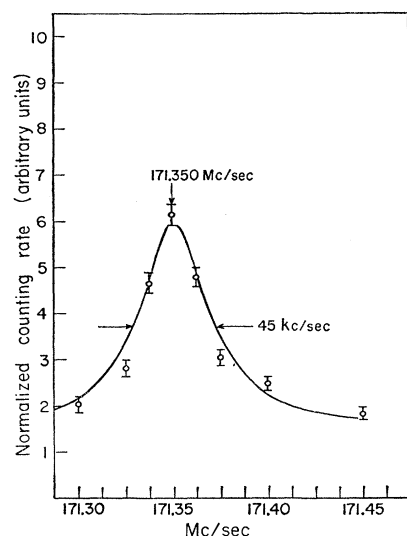


FIG. 4. A resonance corresponding to the transition $F, m = \frac{3}{2}, -\frac{3}{2} \leftrightarrow \frac{3}{2}, -\frac{3}{2}$ in the $^2D_{3/2}$ electronic state of Y^{90} at $H = 32.5$ gauss.

was very small. The correct resonant frequency and other characteristics of the σ -type line were checked with K^{39} using the transition $F, m = 2, -1 \leftrightarrow 1, -1$.

The final results in which routine HYPERFINE has varied the parameters a , b , and g_I to fit all observed resonances are shown in Tables III and IV. When both positive and negative starting values were used, g_I converged to the same negative value in each electronic state.

The value of g_I calculated in this manner provides an independent check on the value calculated with the aid of the Fermi-Segrè formula and the interaction constants

of Y^{89} . The uncertainty in the $^2D_{3/2} g_I$ measurement is very large because the significant π transition for this measurement occurs at only 32.5 gauss. The $^2D_{3/2}$ state gives greater accuracy because here the significant transitions occur in the region of 120 gauss.

The small value of the χ^2 reflects the conservative errors placed on the experimental resonance frequencies. Because the computer uncertainty in each parameter is the standard deviation of that parameter, there should be a 95% probability (for a normal distribution) that the true value lies within two standard deviations of the measured value. With this uncertainty, then, the meas-

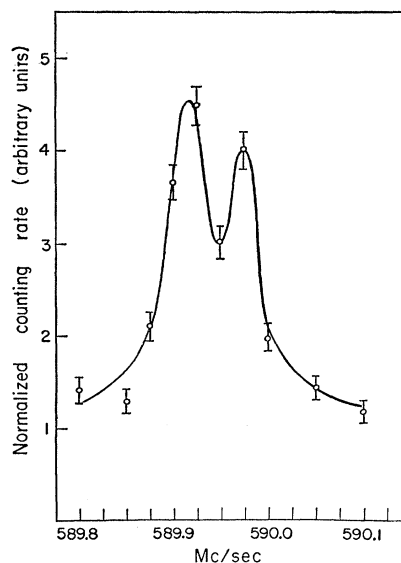


FIG. 5. A resonance corresponding to the transition $F, m = \frac{5}{2}, \frac{3}{2} \leftrightarrow \frac{5}{2}, \frac{3}{2}$ in the $^2D_{3/2}$ electronic state of Y^{90} at $H = 263.2$ gauss.

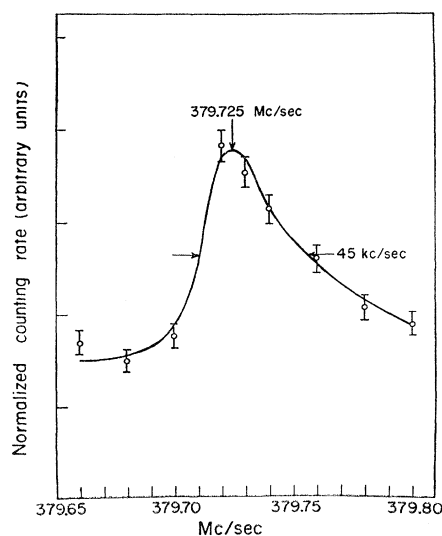


FIG. 6. A resonance corresponding to the transition $F, m = \frac{3}{2}, -\frac{1}{2} \leftrightarrow \frac{3}{2}, \frac{1}{2}$ in the $^2D_{3/2}$ electronic state of Y^{90} at $H = 127.0$ gauss.

TABLE III. Summary of Y⁹⁰ data for the ²D_{3/2} electronic state.

	Comparing isotope $\text{Y}^{89}, {}^2\text{D}_{3/2}, I=\frac{1}{2}$ $g_J=-0.79927$ $g_I=-1.49037\times 10^{-4}$ $a=-57.217$ Mc/sec					Calibrating isotope $\text{Rb}^{85}, {}^2\text{S}_{1/2}, I=\frac{5}{2}$ $g_J=-2.00238$ $g_I=2.93704\times 10^{-4}$ $\Delta\nu=3035.735$ Mc/sec							
	a (Mc/sec) -169.749	δa (Mc/sec) 0.003	b (Mc/sec) -21.602	δb (Mc/sec) 0.013	$g_I\times 10^4$ -4.89	$\delta g_I\times 10^4$ 0.35	χ^2 9.4						
Calibrating isotope	ν_c (Mc/sec)	$\delta\nu_c$ (Mc/sec)	H (gauss)	δH (gauss)	F_1	m_1	F_2	m_2	ν_{obs} (Mc/sec)	$\delta\nu_{\text{obs}}$ (Mc/sec)	Residual (Mc/sec)	Weight factor	
Rb^{85}	4.034	0.040	8.585	0.084	$\frac{7}{2}$	$\frac{5}{2}$	$\frac{7}{2}$	$\frac{3}{2}$	4.131	0.030	-0.013	387.4	
Rb^{85}	7.905	0.040	16.718	0.084	$\frac{7}{2}$	$\frac{5}{2}$	$\frac{7}{2}$	$\frac{3}{2}$	8.101	0.045	-0.014	270.2	
Rb^{85}	50.724	0.085	100.406	0.156	$\frac{7}{2}$	$\frac{5}{2}$	$\frac{7}{2}$	$\frac{3}{2}$	51.480	0.150	-0.078	33.6	
Rb^{85}	179.192	0.150	300.127	0.199	$\frac{7}{2}$	$\frac{5}{2}$	$\frac{7}{2}$	$\frac{3}{2}$	175.600	0.200	-0.178	16.8	
Rb^{85}	50.520	0.130	100.032	0.238	$\frac{5}{2}$	$\frac{3}{2}$	$\frac{5}{2}$	$\frac{1}{2}$	48.400	0.300	-0.108	9.3	
Rb^{85}	2.146	0.040	4.581	0.085	$\frac{5}{2}$	$\frac{3}{2}$	$\frac{5}{2}$	$\frac{3}{2}$	612.480	0.100	-0.103	99.3	
Rb^{85}	152.225	0.060	263.189	0.085	$\frac{5}{2}$	$\frac{3}{2}$	$\frac{5}{2}$	$\frac{3}{2}$	589.940	0.040	0.031	625.0	
Rb^{85}	152.239	0.090	263.209	0.127	$\frac{5}{2}$	$\frac{3}{2}$	$\frac{5}{2}$	$\frac{3}{2}$	589.900	0.040	-0.009	625.0	
Rb^{85}	2.642	0.040	5.636	0.085	$\frac{3}{2}$	$-\frac{1}{2}$	$\frac{5}{2}$	$\frac{1}{2}$	408.920	0.150	-0.112	42.9	
Rb^{85}	4.765	0.040	10.129	0.084	$\frac{3}{2}$	$-\frac{1}{2}$	$\frac{5}{2}$	$\frac{1}{2}$	407.400	0.150	-0.123	42.9	
Rb^{85}	65.581	0.045	127.044	0.079	$\frac{3}{2}$	$-\frac{1}{2}$	$\frac{5}{2}$	$\frac{1}{2}$	379.725	0.015	0.005	4444.4	
Rb^{85}	65.680	0.050	127.218	0.088	$\frac{3}{2}$	$-\frac{1}{2}$	$\frac{5}{2}$	$\frac{1}{2}$	379.720	0.040	0.000	625.0	
Rb^{85}	12.062	0.045	25.339	0.093	$\frac{3}{2}$	$\frac{1}{2}$	$\frac{5}{2}$	$\frac{1}{2}$	407.375	0.175	-0.100	32.4	
Rb^{85}	104.443	0.140	191.807	0.222	$\frac{3}{2}$	$\frac{1}{2}$	$\frac{5}{2}$	$\frac{1}{2}$	363.140	0.040	-0.004	625.0	
Rb^{85}	11.923	0.060	25.053	0.124	$\frac{3}{2}$	$-\frac{1}{2}$	$\frac{5}{2}$	$-\frac{1}{2}$	412.750	0.100	-0.004	99.4	
Rb^{85}	2.485	0.070	5.302	0.149	$\frac{3}{2}$	$\frac{1}{2}$	$\frac{5}{2}$	$-\frac{1}{2}$	412.620	0.200	0.087	23.8	
Rb^{85}	58.357	0.065	114.232	0.116	$\frac{3}{2}$	$\frac{1}{2}$	$\frac{5}{2}$	$-\frac{1}{2}$	424.780	0.010	0.002	10 000.0	
Rb^{85}	2.189	0.040	4.673	0.085	$\frac{3}{2}$	$-\frac{3}{2}$	$\frac{5}{2}$	$-\frac{1}{2}$	410.260	0.200	-0.082	25.0	
Rb^{85}	2.330	0.100	4.973	0.213	$\frac{3}{2}$	$-\frac{3}{2}$	$\frac{5}{2}$	$-\frac{1}{2}$	410.150	0.200	-0.163	24.7	
Rb^{85}	2.659	0.040	5.672	0.085	$\frac{3}{2}$	$-\frac{3}{2}$	$\frac{5}{2}$	$-\frac{1}{2}$	410.200	0.200	-0.048	25.0	
Rb^{85}	4.770	0.040	10.139	0.084	$\frac{3}{2}$	$-\frac{3}{2}$	$\frac{5}{2}$	$-\frac{1}{2}$	409.700	0.200	-0.202	25.0	
Rb^{85}	9.423	0.035	19.880	0.073	$\frac{3}{2}$	$-\frac{3}{2}$	$\frac{5}{2}$	$-\frac{1}{2}$	409.588	0.010	-0.004	9999.9	
Rb^{85}	11.860	0.040	24.923	0.082	$\frac{3}{2}$	$-\frac{3}{2}$	$\frac{5}{2}$	$-\frac{1}{2}$	409.670	0.050	0.003	398.9	
Rb^{85}	2.485	0.070	5.302	0.149	$\frac{3}{2}$	$-\frac{1}{2}$	$\frac{5}{2}$	$-\frac{3}{2}$	413.700	0.100	0.166	65.1	
Rb^{85}	4.160	0.040	8.852	0.084	$\frac{3}{2}$	$-\frac{3}{2}$	$\frac{5}{2}$	$-\frac{5}{2}$	417.375	0.175	0.183	29.1	

ured values of the interaction constants and g_I are

$$^2D_{3/2} \text{ state: } a = -169.749(7) \text{ Mc/sec,}$$

$$b = -21.602(27) \text{ Mc/sec,}$$

$$g_I = -4.9(7) \times 10^{-4},$$

$$^2D_{5/2} \text{ state: } a = -85.258(6) \text{ Mc/sec,}$$

$$b = -29.716(38) \text{ Mc/sec,}$$

$$g_I = -9(6) \times 10^{-4}.$$

From these values for a and b , the zero-field hyperfine-structure separations are

$$^2D_{3/2} \text{ state: } \Delta\nu_{1/2-3/2} = 235.722(26) \text{ Mc/sec,}$$

$$\Delta\nu_{3/2-5/2} = 410.871(24) \text{ Mc/sec,}$$

$$\Delta\nu_{5/2-7/2} = 613.023(34) \text{ Mc/sec,}$$

$$^2D_{5/2} \text{ state: } \Delta\nu_{1/2-3/2} = 114.515(19) \text{ Mc/sec,}$$

$$\Delta\nu_{3/2-5/2} = 198.287(24) \text{ Mc/sec,}$$

$$\Delta\nu_{5/2-7/2} = 293.203(22) \text{ Mc/sec,}$$

$$\Delta\nu_{7/2-9/2} = 403.719(37) \text{ Mc/sec.}$$

From Eqs. (9) and (10), the theoretical ratios of the interaction constants are

$$a'/a'' = 0.4253, \quad b'/b'' = 1.3928.$$

From the experimental measurements,

$$a'/a'' = 0.5023, \quad b'/b'' = 1.3756.$$

The large deviation, especially in the ratios of the a 's, suggests a configuration-mixing effect of the type discussed in Sec. II. The electronic configuration that meets the requirements for an effect of this type is the $4d5s6s$ configuration.

With the aid of Eqs. (14)–(18), the dipole interaction constants may be corrected for the effects of configuration mixing. Then—from the nuclear magnetic moment of Y⁸⁹, and interaction constants for both Y⁸⁹ and Y⁹⁰—we obtain the result

$$\mu_I(Y^{90})_{\text{expt}}^{\text{uncorr}} = -1.623(8) \text{ nm,}$$

which is uncorrected for diamagnetic effects. A 0.5% uncertainty has been assigned to the calculated nuclear

TABLE IV. Summary of Y^{90} data for the $^2D_{1/2}$ electronic state.

Calibrating isotope	Comparing isotope				Calibrating isotopes							
	$Y^{89}, ^2D_{1/2}, I=\frac{1}{2}$ $g_J=-1.20028$ $g_I=-1.49037\times 10^{-4}$ $a=-28.749$ Mc/sec				$Rb^{85}, ^2S_{1/2}, I=\frac{1}{2}$ $g_J=-2.00238$ $g_I=2.93704\times 10^{-4}$ $\Delta\nu=3035.735$ Mc/sec				$Rb^{87}, ^2S_{1/2}, I=\frac{3}{2}$ $g_J=-2.00238$ $g_I=9.95359\times 10^{-4}$ $\Delta\nu=6834.685$ Mc/sec			
	a	δa	b	δb	$g_I\times 10^4$		$\delta g_I\times 10^4$		χ^2		Weight factor	
	(Mc/sec)	(Mc/sec)	(Mc/sec)	(Mc/sec)	-8.75		2.88		14.0			
	-85.258	0.003	-29.716	0.019								
ν_c	$\delta\nu_c$	H	δH	F_1	m_1	F_2	m_2	ν_{obs}	$\delta\nu_{obs}$	Residual		
(Mc/sec)	(Mc/sec)	(gauss)	(gauss)					(Mc/sec)	(Mc/sec)	(Mc/sec)		
Rb ⁸⁵	3.990	0.030	8.492	0.063	$\frac{9}{2}$	$\frac{5}{2}$	$\frac{9}{2}$	$\frac{3}{2}$	7.958	0.030	-0.035	221.7
Rb ⁸⁵	8.078	0.030	17.079	0.063	$\frac{9}{2}$	$\frac{5}{2}$	$\frac{9}{2}$	$\frac{3}{2}$	16.190	0.045	-0.013	176.9
Rb ⁸⁵	20.023	0.030	41.534	0.060	$\frac{9}{2}$	$\frac{5}{2}$	$\frac{9}{2}$	$\frac{3}{2}$	40.280	0.105	-0.022	68.0
Rb ⁸⁵	34.889	0.030	70.721	0.058	$\frac{9}{2}$	$\frac{5}{2}$	$\frac{9}{2}$	$\frac{3}{2}$	70.485	0.190	-0.041	25.1
Rb ⁸⁵	64.916	0.030	125.876	0.053	$\frac{9}{2}$	$\frac{5}{2}$	$\frac{9}{2}$	$\frac{3}{2}$	132.150	0.300	-0.258	10.7
Rb ⁸⁷	133.524	0.050	180.438	0.064	$\frac{9}{2}$	$\frac{5}{2}$	$\frac{9}{2}$	$\frac{3}{2}$	199.600	0.750	-0.631	1.8
Rb ⁸⁵	3.946	0.030	8.399	0.063	$\frac{7}{2}$	$\frac{3}{2}$	$\frac{7}{2}$	$\frac{1}{2}$	8.334	0.085	-0.053	88.3
Rb ⁸⁵	8.059	0.030	17.039	0.063	$\frac{7}{2}$	$\frac{3}{2}$	$\frac{7}{2}$	$\frac{1}{2}$	17.235	0.075	0.011	101.9
Rb ⁸⁵	12.000	0.030	25.211	0.062	$\frac{7}{2}$	$\frac{3}{2}$	$\frac{7}{2}$	$\frac{1}{2}$	25.880	0.200	0.088	22.6
Rb ⁸⁵	16.795	0.030	35.016	0.061	$\frac{7}{2}$	$\frac{3}{2}$	$\frac{7}{2}$	$\frac{1}{2}$	36.500	0.200	0.133	22.5
Rb ⁸⁵	24.398	0.030	50.262	0.059	$\frac{7}{2}$	$\frac{3}{2}$	$\frac{7}{2}$	$\frac{1}{2}$	53.540	0.200	0.011	22.4
Rb ⁸⁵	34.568	0.030	70.104	0.058	$\frac{7}{2}$	$\frac{3}{2}$	$\frac{7}{2}$	$\frac{1}{2}$	77.600	0.300	0.213	10.5
Rb ⁸⁷	68.313	0.040	94.816	0.054	$\frac{7}{2}$	$\frac{3}{2}$	$\frac{7}{2}$	$\frac{1}{2}$	109.800	0.300	-0.066	10.5
Rb ⁸⁷	113.131	0.040	154.143	0.052	$\frac{7}{2}$	$\frac{3}{2}$	$\frac{7}{2}$	$\frac{1}{2}$	199.650	0.500	-0.345	3.9
Rb ⁸⁵	4.002	0.035	8.518	0.074	$\frac{5}{2}$	$\frac{1}{2}$	$\frac{5}{2}$	$-\frac{1}{2}$	9.450	0.150	0.023	34.2
Rb ⁸⁵	12.089	0.030	25.395	0.062	$\frac{7}{2}$	$\frac{3}{2}$	$\frac{7}{2}$	$\frac{3}{2}$	405.120	0.080	-0.013	156.1
Rb ⁸⁵	24.993	0.030	51.440	0.059	$\frac{5}{2}$	$\frac{3}{2}$	$\frac{5}{2}$	$\frac{3}{2}$	405.725	0.025	0.007	1597.7
Rb ⁸⁵	25.297	0.310	52.042	0.612	$\frac{7}{2}$	$\frac{3}{2}$	$\frac{7}{2}$	$\frac{3}{2}$	405.725	0.025	-0.002	1386.6
Rb ⁸⁵	4.020	0.040	8.556	0.085	$\frac{5}{2}$	$\frac{1}{2}$	$\frac{7}{2}$	$\frac{1}{2}$	293.435	0.035	-0.016	816.3
Rb ⁸⁵	4.026	0.035	8.568	0.074	$\frac{5}{2}$	$\frac{1}{2}$	$\frac{7}{2}$	$\frac{1}{2}$	293.425	0.075	-0.026	177.8
Rb ⁸⁵	12.146	0.080	25.512	0.165	$\frac{5}{2}$	$\frac{1}{2}$	$\frac{7}{2}$	$\frac{1}{2}$	292.600	0.150	-0.052	44.0
Rb ⁸⁵	1.721	0.030	3.677	0.064	$\frac{3}{2}$	$-\frac{3}{2}$	$\frac{5}{2}$	$-\frac{5}{2}$	200.750	0.150	0.227	41.4
Rb ⁸⁵	1.729	0.040	3.694	0.085	$\frac{3}{2}$	$-\frac{3}{2}$	$\frac{5}{2}$	$-\frac{5}{2}$	200.525	0.100	-0.008	77.2
Rb ⁸⁵	2.278	0.030	4.862	0.064	$\frac{3}{2}$	$-\frac{3}{2}$	$\frac{5}{2}$	$-\frac{5}{2}$	201.545	0.200	0.252	23.9
Rb ⁸⁵	2.845	0.050	6.067	0.106	$\frac{3}{2}$	$-\frac{3}{2}$	$\frac{5}{2}$	$-\frac{5}{2}$	202.100	0.300	0.000	10.5
Rb ⁸⁵	1.672	0.050	3.572	0.106	$\frac{3}{2}$	$-\frac{1}{2}$	$\frac{5}{2}$	$-\frac{3}{2}$	201.550	0.200	0.127	21.0
Rb ⁸⁵	2.845	0.050	6.067	0.106	$\frac{3}{2}$	$-\frac{1}{2}$	$\frac{5}{2}$	$-\frac{3}{2}$	203.650	0.300	0.282	10.4
Rb ⁸⁵	14.250	0.050	29.831	0.102	$\frac{3}{2}$	$-\frac{1}{2}$	$\frac{5}{2}$	$-\frac{3}{2}$	211.860	0.075	0.086	172.0
Rb ⁸⁵	6.382	0.040	13.530	0.084	$\frac{3}{2}$	$-\frac{3}{2}$	$\frac{5}{2}$	$-\frac{3}{2}$	194.650	0.070	-0.010	204.1
Rb ⁸⁵	2.279	0.030	4.864	0.064	$\frac{3}{2}$	$-\frac{1}{2}$	$\frac{5}{2}$	$-\frac{1}{2}$	196.850	0.200	-0.354	24.8
Rb ⁸⁵	23.633	0.040	48.745	0.079	$\frac{3}{2}$	$-\frac{1}{2}$	$\frac{5}{2}$	$-\frac{1}{2}$	176.450	0.050	-0.036	400.0
Rb ⁸⁵	23.676	0.050	48.830	0.099	$\frac{3}{2}$	$-\frac{1}{2}$	$\frac{5}{2}$	$-\frac{1}{2}$	176.480	0.040	-0.006	625.0
Rb ⁸⁵	9.494	0.030	20.027	0.062	$\frac{3}{2}$	$-\frac{3}{2}$	$\frac{5}{2}$	$-\frac{1}{2}$	175.375	0.200	-0.004	24.0
Rb ⁸⁵	15.572	0.030	32.530	0.061	$\frac{3}{2}$	$-\frac{3}{2}$	$\frac{5}{2}$	$-\frac{1}{2}$	171.350	0.015	0.001	4444.4
Rb ⁸⁵	15.574	0.030	32.534	0.061	$\frac{3}{2}$	$-\frac{3}{2}$	$\frac{5}{2}$	$-\frac{1}{2}$	171.350	0.025	0.001	1600.0
Rb ⁸⁵	15.699	0.050	32.788	0.102	$\frac{3}{2}$	$-\frac{3}{2}$	$\frac{5}{2}$	$-\frac{1}{2}$	171.350	0.015	0.000	4414.0

magnetic moment because of assumptions involved in the Fermi-Segrè relation. With the diamagnetic correction factor, $\kappa=1.00359$, given by Kopfermann,¹² we obtain

$$\mu_I(Y^{90})_{\text{expt}}^{\text{corr}} = -1.629(8) \text{ nm.}$$

The uncorrected nuclear electric quadrupole moment can be obtained from Eq. (13). By use of the corrected dipole interaction constants, the quadrupole moment for either electronic state becomes

$$Q(Y^{90})_{\text{expt}}^{\text{uncorr}} = -0.155(3) \text{ b,}$$

which is uncorrected for Sternheimer effects. An estimated 2% uncertainty has been assigned to the nuclear quadrupole moment because of the uncertainty in g_I , and because the ratio of the b 's for the two electronic states differs from the theoretical ratio by 1.2%.

VI. DISCUSSION

The measured value of the nuclear spin was expected for several theoretical reasons. From nuclear shell structure, the 39th proton should be in the $p_{1/2}$ level. The $g_{9/2}$ level is filled at 50, and the next level filled by

neutrons is the $d_{5/2}$ level. Because the neutron is in a level with intrinsic spin and orbital angular momentum parallel, and the proton is in a level with intrinsic spin and orbital angular momentum antiparallel, the total spin of the nuclear ground state according to Nordheim's "strong" rule¹⁸ (or later modifications¹⁹) should be the difference of the individual angular momenta, or $I=2$. Also, since the asymptotic quantum numbers given by Gallagher and Moszkowski are $\Omega_p=\frac{1}{2}$ (parallel spin) and $\Omega_n=\frac{5}{2}$ (antiparallel spin),²⁰ the collective-model coupling rule predicts $I=2$.

In the jj -coupling limit, the single-particle shell model predicts a nuclear moment given by

¹⁸ L. A. Nordheim, *Revs. Modern Phys.* **23**, 322 (1951).

¹⁹ M. H. Brennan and A. M. Bernstein, *Phys. Rev.* **120**, 927 (1960).

²⁰ C. J. Gallagher, Jr., and S. A. Moszkowski, *Phys. Rev.* **111**, 1282 (1958).

$$\mu_s = \frac{1}{2}I(g_p + g_n) + (g_p - g_n) \left[\frac{j_p(j_p+1) - j_n(j_n+1)}{2(I+1)} \right]. \quad (21)$$

If the nuclear g factors for the odd proton and neutron are evaluated from the Schmidt formulas, Eq. (21) predicts $\mu_s = -1.609$ nm. This result agrees remarkably well with the experimental value. The collective model in the limit of strong coupling of the nucleon to the surface predicts a magnetic moment given by

$$\mu_c = (g_n\Omega + g_p)I/(I+1). \quad (22)$$

If one estimates $g_n\Omega$ from the expression given by Gallagher and Moszkowski,²⁰ and takes $g_p \approx Z/A$, the result is $\mu_c = -0.30$ nm. From magnetic-moment considerations, then, the independent-particle shell model appears to be a better representation than the collective model for Y⁹⁰.

(p,n) Cross Sections on Ti⁴⁷, V⁵¹, Cr⁵², Co⁵⁹, and Cu⁶³ from 4 to 6.5 Mev

H. TAKETANI* AND W. PARKER ALFORD

Department of Physics and Astronomy, University of Rochester, Rochester, New York

(Received August 25, 1961)

Absolute (p,n) cross sections have been measured for Ti⁴⁷, V⁵¹, Cr⁵², Co⁵⁹, and Cu⁶³ at energies between 4 and 6.5 Mev. These data plus earlier measurements of the cross section for inelastic proton scattering have been used to estimate total proton absorption cross sections for V⁵¹ and Co⁵⁹. An optical model calculation using parameters giving a good fit to elastic scattering measurements predicts an absorption cross section in good agreement with the measurements for Co⁵⁹. For V⁵¹, some sets of parameters gave good agreement with the measured absorption cross section, but the fit to the elastic scattering data was only fair.

I. INTRODUCTION

ANGULAR distributions of low-energy protons elastically scattered by V, Cr, Fe, and Co have been measured in this laboratory by Preskitt and Alford.¹ In analyzing these results, it was found that the angular distributions for Co could be fitted with an optical model calculation employing a Woods-Saxon potential well.² Good fits to the Co data were obtained for a rather wide range of values for the well depth V_0 , provided that the product $V_0R_0^2$ was held constant, where R_0 is the nuclear radius. The calculated absorption cross sections depended rather sensitively on R_0 , however, and the present measurements were undertaken in an effort to narrow the range of acceptable values of V_0 and R_0 . In the course of the work, measurements were extended to the nuclei Ti⁴⁷, Cr⁵², and Cu⁶³,

and (p,n) cross sections for these nuclei are reported here also.

II. MEASUREMENTS

All measurements were carried out using the external proton beam of the University of Rochester variable-energy cyclotron. The mean energy of the beam was measured in a calibrated analyzer magnet and was known to within 1%. In most of the measurements, the energy spread in the beam was about 100 kev. The targets used are listed in Table I along with their relevant properties. Target thicknesses were determined by weighing, and are accurate to within $\pm 3\%$.

Two procedures were used in carrying out the (p,n) cross-section measurements. For Ti⁴⁷, Cr⁵², and Cu⁶³, the positron activity produced in a foil by the reaction was measured using a method similar to that described by Howe.³ Foils of the element to be studied were mounted in light rigid frames, and a stack of foils placed in a holder behind a beam-defining aperture. A pair of

* Now at the Department of Physics, University of Maryland, College Park, Maryland.

¹ C. A. Preskitt, Jr., and W. P. Alford, *Phys. Rev.* **115**, 389 (1959).

² R. D. Woods and D. S. Saxon, *Phys. Rev.* **95**, 577 (1954).

³ H. A. Howe, *Phys. Rev.* **109**, 2083 (1958).